ISSN 0965-545X, Polymer Science, Series A, 2021, Vol. 63, No. 3, pp. 267–274. © Pleiades Publishing, Ltd., 2021.

POLYMER BLENDS

Crystallization Behavior of Homochiral Polymer in Poly(*L*-lactic acid)/Poly(*D*-lactic acid) Asymmetric Blends: Effect of Melting States

Jun Shao[a,b,c,d,*], Juan Tang[a,b], Shouzhi Pu[a,], and Haoqing Hou[b,c]**

[a]*Jiangxi Key Laboratory of Organic Chemistry, Jiangxi Science and Technology Normal University, Nanchang, Jiangxi, 330013 China*

[b]*College of Chemistry and Chemical Engineering, Jiangxi Normal University, Nanchang, 330022 China*

[c]*Nanofiber Engineering Center of Jiangxi Province, Jiangxi Normal University, Nanchang, 330022 China*

[d]*Key Laboratory of Functional Small Organic Molecule, Ministry of Education and Jiangxi's Key Laboratory of Green Chemistry, Jiangxi Normal University, Nanchang, 330022 China*

**e-mail: jun.shao@juxn.edu.cn*

***e-mail: pushouzhi@tsinghua.org.cn*

Received October 1, 2020; revised December 11, 2020; accepted December 25, 2020

Abstract—Blending of poly(*L*-lactic acid)/poly(*D*-lactic acid) (PLLA/PDLA) leads to the formation of poly(lactide) stereocomplexation (PLA SC), which exhibits higher melting temperature and faster crystallization rate. The crystallization behavior of PLA homochiral crystallization (HC) under the existence of PLA SC was also widely investigated. During the variable processing, the SC with different morphologies would produce, and these SC could exert different influences on the subsequent formation of HC. However, the effects of SC developed in various conditions on the formation of HC are not compared yet and are also not clear until now, and which is important for the application of PLLA/PDLA blends. In this paper, the PDLAs with different molecular weights were blended with PLLA at a weight ratio of PLLA/PDLA 90/10, and the crystallization behaviors of PLLA HC from different conditions were investigated by differential scanning calorimetry (DSC). Results indicated that, incorporating a small amount of PDLA accelerated the formation of PLLA HC significantly regardless of the SC developed from the solution evaporation or the melt. The higher crystallization rate of HC was received in the PLLA/PDLA specimens with lower molecular weight of PDLA. For the specimens crystallized from the partially melting (most of SC developed during solution evaporation), the crystallization rate was higher than that corresponding specimens crystallized from the completely melting state (the SC were produced from the melt). This discrepancy would be due to variable SC morphologies produced during diverse processing.

DOI: 10.1134/S0965545X2103010X

INTRODUCTION

The poly(lactic acid) (PLA) is regard as one of the most promising materials in the twenty first century, which is bio-based, biodegradable, biocompatible, and excellent strength [1–3]. Notwithstanding, the wide application of PLA still encounter some intrinsic bottlenecks, and one of the problems need to solve is the slow crystallization rate [4, 5]. Lots of solutions, such as adding nucleate agents [6–10], blending with other polymers [11, 12], orientation, annealing at proper temperature [13, 14], copolymerization and plasticization [15] were proposed. Due to the chair atom on the lactic acid, there are two cystallizable PLA materials, i.e., poly(*L*-lactic acid) and poly(*D*-lactic acid), which are named as PLLA and PDLA, respectively [16]. Blending of PLLA and PDLA, a novel stereocomplex crystallites (SC) develops [17–19]. According to the latest reports, the melting temperature of SC was 250°C, which is ~80°C higher than that of PLLA or PDLA homochiral crystallites (HC) [20, 21]. And the PLA SC is also reported as an efficient nucleate agent to accelerate the crystallization of HC [22–32]. According to the investigations, the SC produced either from the solution evaporation or from the melting crystallization. Variable morphologies produced when the PLLA/PDLA were experienced different processing. Lots of literatures revealed that, the SC formed efficiently during solution evaporation [20, 33–36], and the SC usually presented with a network structure [37–39]. Crystallized from the melt, the SC with a spherical morphology developed in most of cases [40–44]. The SC with different morphology would exert different influences on the formation of HC. However, the effect of the SC developed in these two cases on the formation of HC was

Table 1. The characterizations of PLLA and PDLA

Code	$M_n \times 10^{-3}$	PDI	T_m, °C
PLLA	107.4	1.5	162.3
PDLA9	9.4	1.7	163.0
PDLA18	18.4	1.7	169.2
PDLA24	23.6	1.6	172.2
PDLA35	35.0	1.6	176.8
PDLA67	67.4	1.8	176.9
PDLA102	102.2	1.6	177.5

not investigated yet, and which would be important for the application of PLLA/PDLA blends. For this purpose, the PDLAs with different molecular weights were synthesized and were blended with commercial PLLA by solution mixing, and the effect of SC developed from the solution evaporation (partially melting) and from the melt (completely melting) on the crystallization behavior of HC was investigated.

EXPERIMENTAL

Materials

Tin (II) 2-ethylhexanoate ($Sn(Oct)_2$, 95%) was bought from Sigma-Aldrich, and was used without purification. The diethylene glycol monomethyl ether (DE) (> 99.5%) was purchased from Aladdin. The dextrorotatory-lactide (D-LA) (optical purity ≥ 99.5%) was kindly supplied by Changchun Sino Biomaterials Co., Ltd. (China). The PDLA was received by ring-opening polymerization of purified D-LA (recrystallized in anhydrous ethyl acetate for three times) at 120°C in anhydrous toluene for 24 h, initiating by DE and catalyzing by $Sn(Oct)_2$ under inert atmosphere. The PDLA with different molecular weights was regulated by the weight ratio of DE/LA [20, 43, 45]. The polymerization was terminated and precipitated by adding a large amount of freezing ethanol into the polymer solution. The precipitated product was dissolved in dichloromethane and precipitated in ethanol again to purify. The PLLA was a commercial grade product which was supplied by Zhejiang Hisun biomaterials Co., Ltd and was purified by dissolving and precipitation as the PDLA. All the purified solid products were dried at 60°C in vacuum to constant weight, and their characterizations were list in Table 1.

Sample Preparation

The PLLA and PDLA were separately dissolved completely in dichloromethane, at a concentration of 12.5 g/L. And then, the solutions were admixed together with a fixed weight ratio, i.e., PLLA/PDLA 90/10. The mixed solutions were stirred intensely for 3 h at room temperature. Finally, the mixed solutions were poured onto petri-dishes and evaporated under room temperature. Further vacuum-drying at 50°C for 72 h were carried out for these specimens to remove residual solvent. In the PLLA/PDLA specimens, the neat PLLA was coded as L162, and the PLLA/PDLA specimens with different molecular weights of PDLA were labeled as D-XX, where the number after L was its melting temperature, while the number after D was the number average weight of PDLA in the specimens.

Characterizations

The number average molecular weights M_n and molecular weight distributions (PDI) were evaluated by a Waters gel permeation chromatography system (GPC), which equipped with two Styragel HR gel columns, i.e., HR2 and HR4. Chloroform ($CHCl_3$) was used as the eluent, and the flow rate of eluent fixed at 1 mL/min. The measurement was carried out at 35°C. Monodispersed polystyrene standards purchased from Waters Co. with a molecular weight ranging from 1790 to 2.0×10^5 g/mol were used to generate the calibration curve.

The crystalline structures were analyzed by a wide-angle X-ray diffraction (WAXD). The WAXD profiles were recorded on a Bruker D8 Advance X-ray diffractometer, adopting a CuK_α radiation source (λ = 0.154 nm, 40 kV, 25 mA). The scanning angle ranged from $2\theta = 10°$ to 30° at a scanning speed of 1°/min.

The thermal properties were studied by a differential scanning calorimetry (DSC) (Mettler Toledo DSC3) under a 20 mL/min nitrogen gas flow. The first heating of all the specimens were performed at a heating rate of 10 K/min from 25–250°C. During the non-isothermal crystallization, the scanning ran at a cooling rate of –2.5 K/min from a fixed temperature to the room temperature. For the isothermal crystallization protocol, the specimens were cooled at a rate of –50 K/min to a given temperature, i.e., 130°C, and kept at this temperature for 120 min to crystallization efficiently. The temperature and heat flow were calibrated with standard indium (T_m = 156.6°C, ΔH = 28.5 J/g) to ensure the reliability of data obtained.

The polarized optical microscope (POM, Carl Zeiss, Axio Imager A2m) equipped with a heating-cooling stage and temperature controller (Linkam THMS-600) was used to observe the morphology of SC. The specimens were heated from room temperature to 250°C at a rate of 30 K/min, and held for 1 min to ensure the specimens were melted completely, and then, the specimens were cooled at a rate of 100 K/min to 130°C and held at this temperature to observe the morphology. Nitrogen gas was purged throughout the hot stage in the whole measurements.

The scanning electron microscopes (SEM, TESCAN, Vega3) was employed to observed the morphologies of the specimens, and the specimens were coated with gold (Au) under vacuum before observation.

RESULTS AND DISCUSSION

Crystallization Behavior of PLLA/PDLA as Solution Casting

The WAXD patterns of PLLA/PDLA original blends with various molecular weights were displayed in Fig. 1a. Where the diffraction peaks located at 14.8°, 16.9°, 19.1°, and 22.5° were assigned to the 010, 200/110, 203, and 210 plane reflection of PLLA α crystallites (HC), respectively [23, 46]. And the diffraction peaks at 12.1°, 21.0°, and 24.0° were belonged to 110, 300, and 220 reflection of PLA SC [22, 47–49]. For the L162 specimen, a weak diffraction at 16.9° was found, which indicated that the neat PLLA did not from crystallites efficiently during solvent evaporation. For the PLLA/PDLA blends, the diffraction peaks assigned to HC enhanced obviously, and the diffraction belonged to SC was also observed, which indicated that more content of crystallites developed in the blends during solution evaporation. The DSC of the casted PLLA/PDLA specimens were shown in Fig. 1b, all the specimens displayed a glass transition temperature around 62°C. For the L162, an apparent cold crystallization peak was detected at 105°C, while no obvious cold crystallization peak was detected in the PLLA/PDLA blends, which implied that the PLLA did not form crystallites efficiently, while the PLLA/PDLA developed crystallites efficiently during solvent evaporation. An endothermic peak was found at 162°C in the L162, it was ascribed to the melting peak of PLLA HC. For the PLLA/PDLA blends, besides the melting signals of PLLA HC, another endothermic peak was found ~215°C, which belonged to the melting of PLA SC. The melting temperature of SC (T_{SC}) increased at first, and then decreased with enlarging the molecular weight of PDLA. Both the WAXD and DSC results hinted that, the neat L162 did not crystallize efficiently during solution evaporation. After incorporating 10 wt % PDLA into L162, the SC produced preferentially during solution casting, and these formed SC acted as nucleate agent for the subsequently formation of HC and improved the crystallization rate of HC.

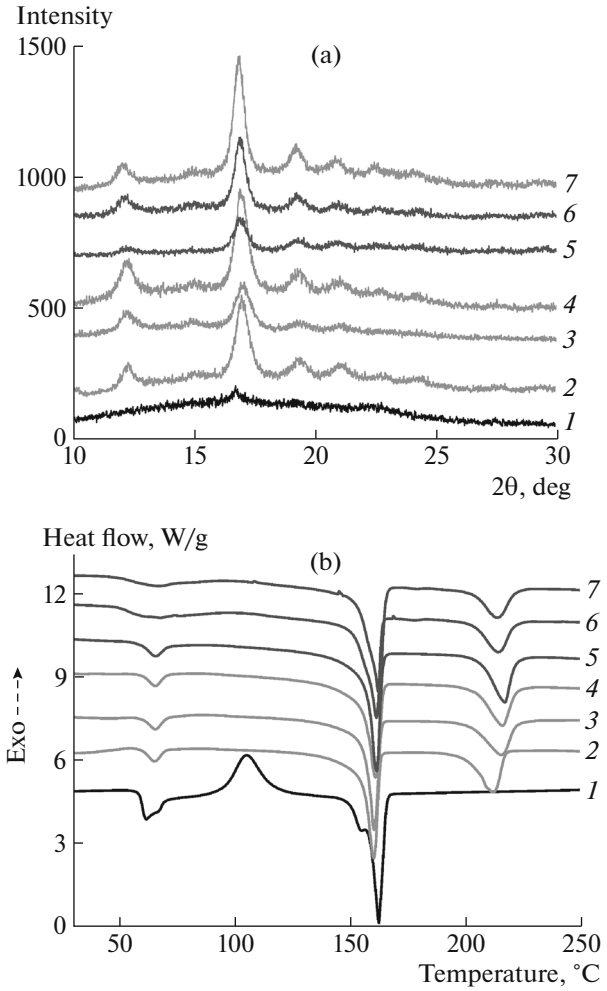

Fig. 1. (a) The WAXD and (b) DSC of the original PLLA/PDLA specimens: (*1*) L162, (*2*) D-9, (*3*) D-18, (*4*) D-24, (*5*) D-35, (*6*) D-67, (*7*) D-102.

Crystallization Behavior from the Partially Melting State

According to the DSC displayed in Fig. 1b, the melting peak of PLLA HC (T_{HC}) was ~162°C, and the T_{SC} was ~215°C. In addition, both HC and SC in the PLLA/PDLA specimens crystallized efficiently during solution evaporation. When the specimens were heated to 190°C, and kept at this temperature for 5 min, the PLLA HC would be melted completely, while the content of SC hardly changed. Thus, when the specimens were cooled to 20°C at a rate of −2.5 K/min, the crystallization signals of the specimens should be limited to the formation of HC under the existence of SC (most of the SC developed during solution evaporation). And these cooling curves were exhibited in Fig. 2. For the L162, a weak crystallization signal was found around at 109°C during cooling, while obvious crystallization signals were observed at higher temperature for all the PLLA/PDLA specimens, and the crystallization enthalpy was around ~20 J/g for all the blends, which were much higher than that value of L162. This result indicated that the formation of HC was apparently accelerated under the existence of SC.

After annealing at 190°C for 5 min, the specimens were cooled at a fast rate to 130°C (−50 K/min), and crystallized at this temperature for 120 min. The crystallization curves were displayed in Fig. 3a. A wide and weak endothermic peak was observed in the L162, while distinct and sharp crystallization peak were detected in all the PLLA/PDLA blends. Figure 3b showed the crystallinity as a function of time (t) for PLLA HC. It could be seen that all the curves exhibited sigmoidal shapes. For the L162, the crystalliza-

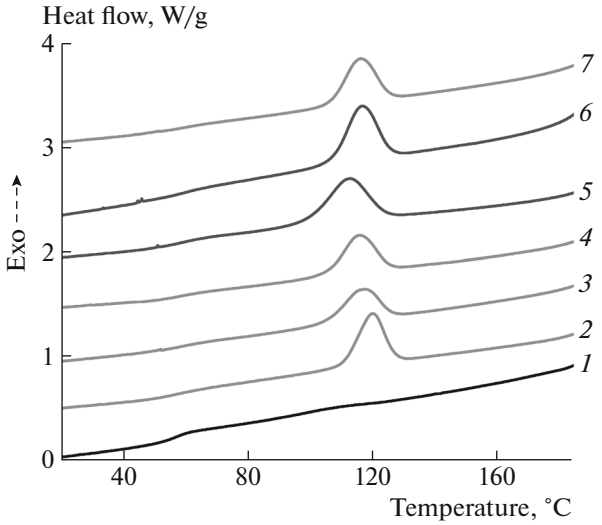

Fig. 2. The DSC cooling curves of PLLA/PDLA blends (from 190°C): (*1*) L162, (*2*) D-9, (*3*) D-18, (*4*) D-24, (*5*) D-35, (*6*) D-67, (*7*) D-102.

tion finished ~80 min. In the case of PLLA/PDLA specimens, the crystallization finished in a short time, ~20 min. The crystallization time tended to increase as elevating the molecular weight of PDLA, which indicated that the crystallization rates decreased with the molecular weight of PDLA (the half-time of crystallization ($t_{1/2}$) of the specimens were list in Table 2).

The Avrami Equation was employed to analyze the crystallization kinetics of the formation of PLLA HC [50, 51]. The Equation was expressed as followed:

$$\ln[-\ln(1 - X_t)] = \ln K + n\ln t. \quad (1)$$

In Equation (1), the X_t was the degree of crystallinity at a given time t, and the X_t could be calculated as the ratio between the area of exothermic peak at time t and the total measured area of crystallization [52]. The K was the Avrami crystallization rate constant, t was the crystallization time. The n was the Avrami index, which correlated to the nucleation mechanism and growth dimension.

The plots of $\ln[-\ln(1 - X_t)]$ versus $\ln t$ for PLLA HC were shown in Fig. 3c. The X_t from 3 to 30% was employed (avoiding the second crystallization) when calculated the slopes and intercepts [53, 54]. All the crystallization kinetic curves exhibited good linearity, and the values of n and $\ln K$ were list in Table 2. The n of L162 was 2, indicating that the crystallites mainly developed with two dimensional structure when crystallization at 130°C. For the PLLA/PDLA blends, the n values varied from 2.4 to 2.9, and they were higher than L162, implying that more than one crystallization mechanisms were conducted in the blends, the SC could act as the heterogeneous nucleation agents, and led to parts of HC developed crystallites with three dimensional structure. The lnK increased obviously

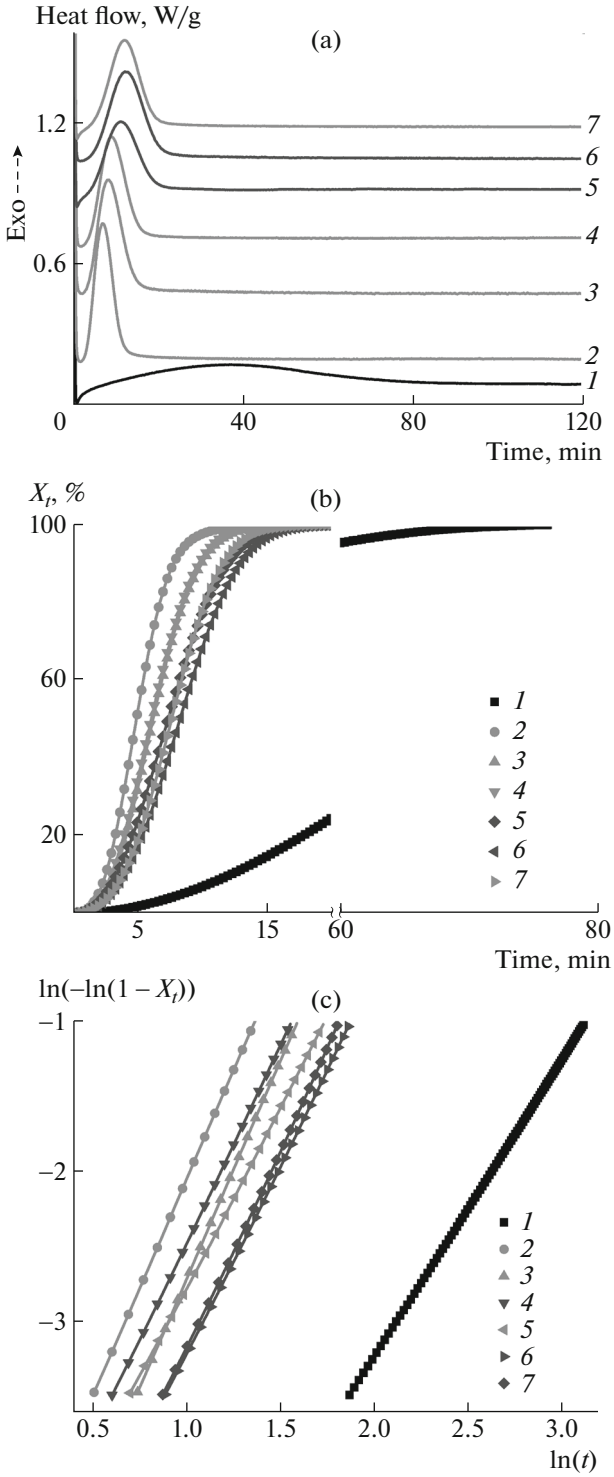

Fig. 3. (a) The crystallization, (b) integral and (c) the crystallization kinetic curves of the PLLA/PDLA specimens (from 190°C): (*1*) L162, (*2*) D-9, (*3*) D-18, (*4*) D-24, (*5*) D-35, (*6*) D-67, (*7*) D-102.

after the L162 was blended with PDLA. As increasing molecular weight of PDLA, the $\ln K$ tended to reduced. The $1/t_{1/2}$ presented similar regularity as $\ln K$.

Crystallization Behavior from the Completely Melt State

As the T_{SC} of the PLLA/PDLA specimens was ~215°C, when the specimens were heated to 250°C, both the SC and HC could be melted completely. During crystallization form the melt, the SC would be preferentially developed due to the stronger interaction among isomer polymers and the higher degree of supercooling of the stereocomplex crystallites. The cooling DSC curves from 250°C were list in Fig. 4. It found that weak crystallization signals were detected in the L162, and a wide crystallization peak was observed in the D-9. For the D-18, two crystallization peaks were found, the higher one should be ascribed to the formation of SC, and the lower one was belonged to the development of HC [32]. As the molecular weight of PDLA further increasing, only one crystallization peak was observed in the specimen, and the crystallization temperature tended to decline.

The isothermal crystallization curves (from 250°C) of the PLLA/PDLA were exhibited in Fig. 5a, and it can be seen that the crystallization of L162 specimen consumed ~90 min. After the PDLA was blended with L162, the crystallization time declined sharply. In the D-9, D-18, D-24, D-35 specimens, two crystallization peaks were observed during crystallization, the signals appeared at the earlier stage was assigned to the formation of PLA SC, and the subsequently crystallization peak was ascribed to the development of PLLA HC. The integral curve of PLLA HC was displayed in Fig. 5b. As two crystallization peaks were found in the D-9, D-18, D-24, D-35 specimens, the signals appeared at the later stage were employed when calculated the integral of PLLA HC. For the D67 and D102 specimens, only one crystallization peak was found, which should combine with signals of the formation of SC and HC, and they were also list in the Fig. 5b. It can be seen that, the crystallization time declined after incorporating PDLA, which indicated that the SC accelerated the formation of HC. As the molecular weight of PDLA increased from 9 to 35 kg/mol, the crystallization time tended to increase. The crystallization time decreased again with further increasing the molecular weight of PDLA (the $t_{1/2}$ was list in Table 3), which should be due to the reason that only one crystallization peak was found, and the signals combined with SC and HC. The crystallization kinetic curves were presented in Fig. 5c, and the kinetic parameters were list in Table 3, similar with the cases in Table 2, the n value for PLLA was ~2, and ~2.5 for all the binary blends.

The $t_{1/2}$ values of PLLA HC with different annealing history were presented in Fig. 6. It can be seen that, the $t_{1/2}$ of the two annealing processes exhibited similar regularity, i.e., the crystallization time decreased sharply after a small amount of PDLA incorporated into the PLLA matrix. In addition, the crystallization time of PLLA/PDLA specimens increased at first,

Table 2. The kinetic parameters of PLLA/PDLA at 130°C (from 190°C)

Code	n	$\ln K$, $\min^{-n}$	$t_{1/2}$, min
L162	2.0	−7.2	31.0
D-9	2.9	−5.0	5.0
D-18	2.9	−5.6	6.2
D-24	2.6	−5.1	6.1
D-35	2.4	−5.2	7.4
D-67	2.5	−5.7	8.3
D-102	2.6	−5.8	7.7

Table 3. The kinetic parameters of PLLA/PDLA at 130°C (from 250°C)

Code	n	$\ln K$, $\min^{-n}$	$t_{1/2}$, min
L162	1.9	−7.1	33.4
D-9	2.6	−6.2	9.4
D-18	2.3	−6.5	13.5
D-24	2.3	−7.1	17.5
D-35	2.3	−6.8	16.8
D-67	2.4	−6.7	12.6
D-102	2.8	−7.8	12.5

and then reduced with enlarging the molecular weight of PDLA. However, when the specimens were annealed at 190°C, the crystallization rate was higher than that specimens annealed at 250°C, this divergence would be ascribed to the reason that the SC developed with different morphologies. For the specimens annealed at 190°C, most of the SC were devel-

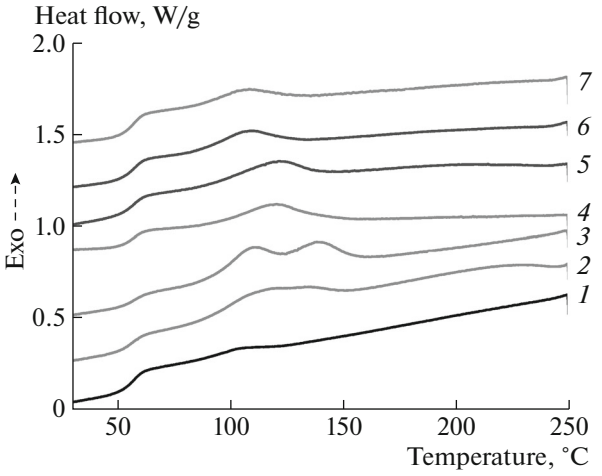

Fig. 4. The DSC cooling curves of PLLA/PDLA blends (from 250°C): (*1*) L162, (*2*) D-9, (*3*) D-18, (*4*) D-24, (*5*) D-35, (*6*) D-67, (*7*) D-102.

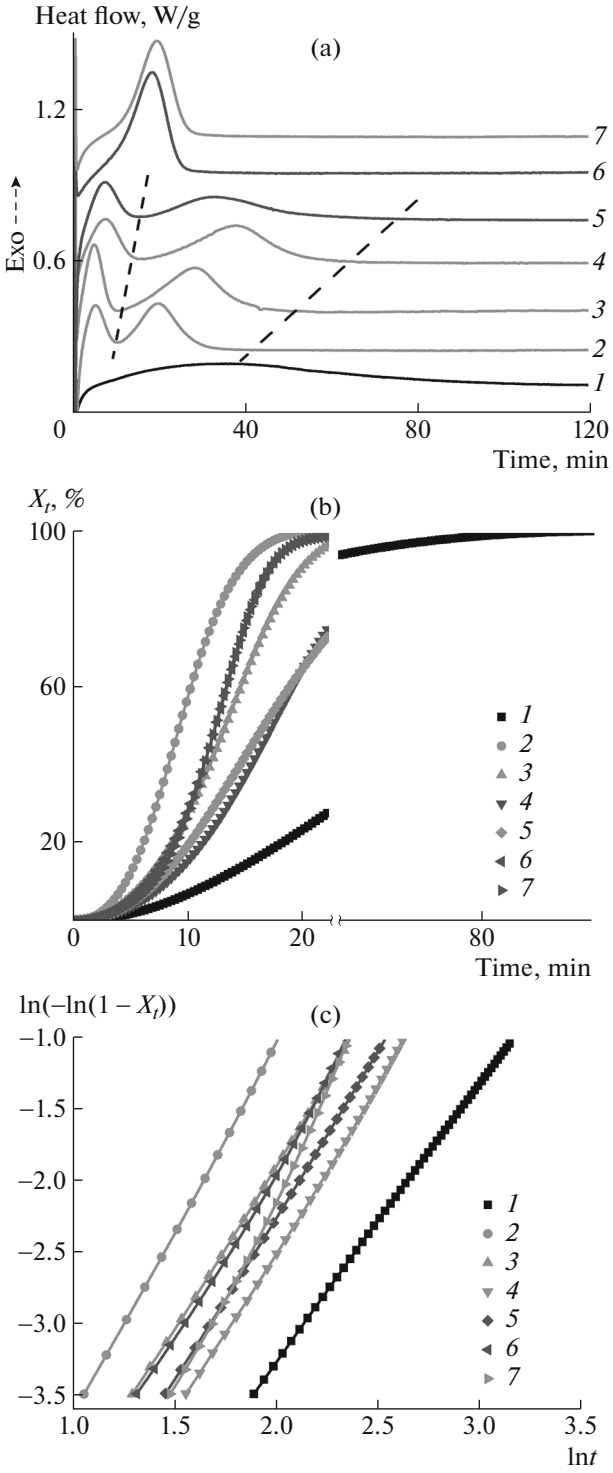

Fig. 5. (a) Crystallization, (b) integral, and (c) kinetic curves of the PLLA/PDLA specimens (from 250°C): (*1*) L162, (*2*) D-9, (*3*) D-18, (*4*) D-24, (*5*) D-35, (*6*) D-67, (*7*) D-102.

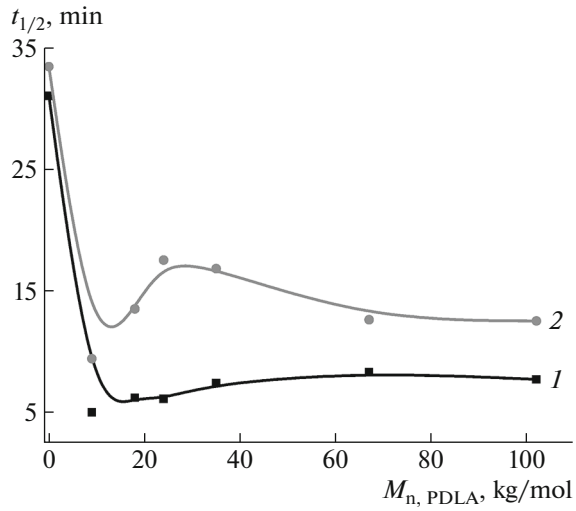

Fig. 6. The $t_{1/2}$ of the PLLA/PDLA blends annealing at different conditions: (*1*) 190–130°C, (*2*) 250–130°C.

oped during solvent evaporation, and the SC with network morphology produced evenly in the specimens (Fig. 7a), this network accelerated the formation of PLA HC efficiently [37, 38]. For the samples annealed at 250°C, the SC were formed during annealing at 130°C, as the higher degree of supercooling, the isomer polymers cannot interdiffuse on a large scale, which interacted with isomers nearby. The stereocomplex crystallites mainly developed as small spherical shape (Fig. 7b), and these spherulites also accelerated the formation of HC, but a relative lower acceleration effect than that of network [40].

CONCLUSIONS

In this study, the synthesized PDLA was blended with commercial PLLA with a weight ratio of PLLA/PDLA 90/10. After the SC with various morphologies was produced, the formation of HC under the existence of SC was investigated. And the following conclusions were made. (i) Compared to neat PLLA specimen, the incorporating of PDLA accelerated the formation of PLA HC regardless of molecular weight of PDLA and morphologies of PLA SC. As the molecular weight of PDLA increasing, the crystallization rate of PLA HC tended to decreased. (ii) When the SC developed from the solution evaporation, the SC with network structure produced, while the spherical shape was observed when the SC crystallized from the melt. The SC network exhibited better acceleration for the development of PLA HC. (iii) This investigation indicated that the SC exhibited different morphologies would have diverse crystallization enhancements, and would provide instruction of application of PLA SC.

FUNDING

This work was financially supported by the National Natural Science Foundation of China (nos. 51403089, 21574060, and 21374044), the Major Special Projects of

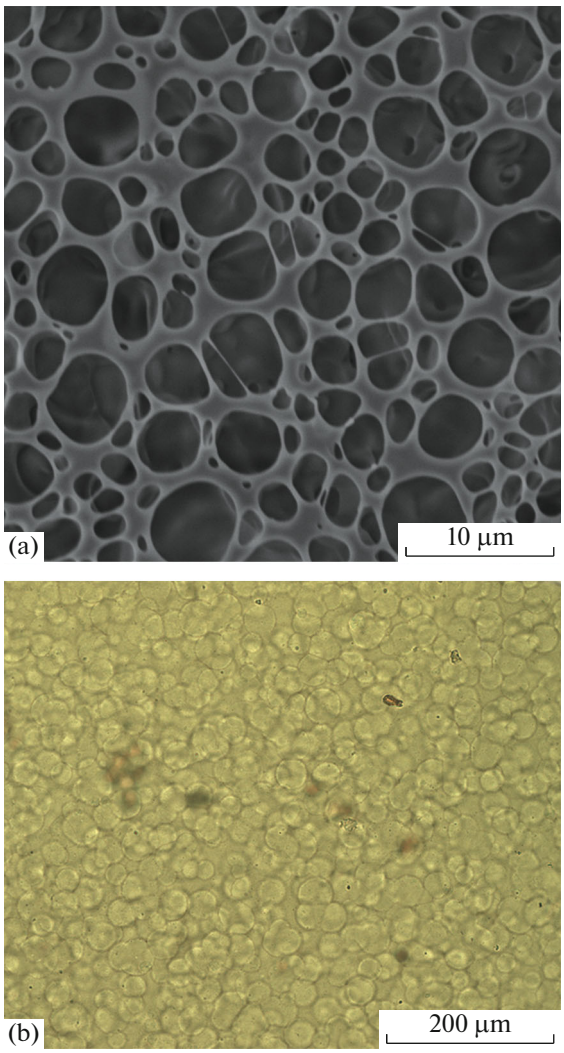

Fig. 7. (a) The SEM of D-24 (the specimen was immersed in dichloromethane for 5 min to dissolve the PLLA HC and amorphous polymers, and then were dried in vacuum), (b) The POM of D-24 (the specimen was heated to 250°C, held for 1 min, and then were cooled to 130°C, and held for 4 min).

Jiangxi Provincial Department of Science and Technology (no. 20114ABF05100), the Project of Jiangxi Provincial Department of Education (no. GJJ170229), the Technology Plan Landing Project of Jiangxi Provincial Department of Education (no. GCJ2011-243), the China Postdoctoral Science Foundation (no. 2019M652282), the Postdoctoral Science Foundation of Jiangxi Province (no. 2018KY37), the Science Foundation for Excellent Young Scholars of Jiangxi Province (no. 20202ZDB01003), the Science foundation of Jiangxi Province (no. 20202BAB203008).

CONFLICT OG INTEREST

The authors declare that they have no conflict of interest.

REFERENCES

1. R. E. Drumright, P. R. Gruber, and D. E. Henton, Adv. Mater. **12**, 1841 (2000).
2. D. Garlotta, J. Polym. Environ. **9**, 63 (2001).
3. X. Pang, X. L. Zhuang, Z. H. Tang, and X. S. Chen, Biotechnol. J. **5**, 1125 (2010).
4. K. Madhavan Nampoothiri, N. R. Nair, and R. P. John, Bioresour. Technol. **101**, 8493 (2010).
5. R. M. Rasal, A. V. Janorkar, and D. E. Hirt, Prog. Polym. Sci. **35**, 338 (2010).
6. W. Y. Zhou, B. Duan, M. Wang, and W. L. Cheung, J. Appl. Polym. Sci. **113**, 4100 (2009).
7. Q. Xing, X. Q. Zhang, X. Dong, G. M. Liu, and D. J. Wang, Polymer **53**, 2306 (2012).
8. R. G. Liao, B. Yang, W. Yu, and C. X. Zhou, J. Appl. Polym. Sci **104**, 310 (2007).
9. M. Penco, G. Spagnoli, I. Peroni, M. A. Rahman, M. Frediani, W. Oberhauser, and A. Lazzeri, J. Appl. Polym. Sci. **122**, 3528 (2011).
10. Y. T. Shieh, Y. K. Twu, C. C. Su, R. H. Lin, and G. L. Liu, J. Polym. Sci., Part B: Polym. Phys. **48**, 983 (2010).
11. H. W. Xiao, W. Lu, and J. T. Yeh, J. Appl. Polym. Sci. **112**, 3754 (2009).
12. M. Li, D. Hu, Y. Wang, and C. Shen, Polym. Eng. Sci. **50**, 2298 (2010).
13. M. L. Di Lorenzo, Eur. Polym. J. **41**, 569 (2005).
14. M. L. Di Lorenzo, Macromol. Symp. **234**, 176 (2006).
15. H. Xiao, W. Lu, and J. T. Yeh, J. Appl. Polym. Sci. **113**, 112 (2009).
16. K. Majerska and A. Duda, J. Am. Chem. Soc. **126**, 1026 (2004).
17. Y. Ikada, K. Jamshidi, H. Tsuji, and S. H. Hyon, Macromolecules **20**, 904 (1987).
18. T. Biela, A. Duda, and S. Penczek, Macromolecules **39**, 3710 (2006).
19. A. Michalski, M. Brzezinski, G. Lapienis, and T. Biela, Prog. Polym. Sci. **89**, 159 (2019).
20. J. Shao, S. Xiang, X. Bian, J. Sun, G. Li, and X. Chen, Ind. Eng. Chem. Res. **54**, 2246 (2015).
21. X. Hu, J. Shao, D. Zhou, G. Li, J. Ding, and X. Chen, J. Appl. Polym. Sci. **134**, e44626 (2017).
22. C. Feng, Y. Chen, J. Shao, and H. Hou, Ind. Eng. Chem. Res. **59**, 8480 (2020).
23. J. Shao, J. Sun, X. Bian, Y. Cui, Y. Zhou, G. Li, and X. Chen, Macromolecules **46**, 6963 (2013).
24. S. C. Schmidt and M. A. Hillmyer, J. Polym. Sci., Part B: Polym. Phys. **39**, 300 (2001).
25. S. Brochu, R. E. Prudhomme, I. Barakat, and R. Jerome, Macromolecules **28**, 5230 (1995).
26. H. Yamane, K. Sasai, Polymer **44**, 2569 (2003).
27. K. S. Anderson and M. A. Hillmyer, Polymer **47**, 2030 (2006).
28. H. Tsuji, H. Takai, N. Fukada, and H. Takikawa, Macromol. Mater. Eng. **291**, 325 (2006).
29. H. Tsuji, H. Takai, and S. K. Saha, Polymer **47**, 3826 (2006).
30. J. Narita, M. Katagiri, and H. Tsuji, Macromol. Mater. Eng. **296**, 887 (2011).

31. N. Rahman, T. Kawai, G. Matsuba, K. Nishida, T. Kanaya, H. Watanabe, H. Okamoto, M. Kato, A. Usuki, M. Matsuda, K. Nakajima, and N. Honma, Macromolecules **42**, 4739 (2009).
32. J. Sun, H. Yu, X. Zhuang, X. Chen, and X. Jing, J. Phys. Chem. B **115**, 2864 (2011).
33. J. Shao, J. Sun, X. Bian, Y. Cui, G. Li, and X. Chen, J. Phys. Chem. B **116**, 9983 (2012).
34. H. Tsuji, S. H. Hyon, and Y. Ikada, Macromolecules **24**, 5651 (1991).
35. H. Tsuji, F. Horii, S. H. Hyon, and Y. Ikada, Macromolecules **24**, 2719 (1991).
36. H. Tsuji, S. H. Hyon, and Y. Ikada, Macromolecules **25**, 2940 (1992).
37. J. Shao, L. Xu, S. Pu, and H. Hou, Polym. Bull. (2020). https://doi.org/10.1007/s00289-020-03103-9
38. X. F. Wei, R. Y. Bao, Z. Q. Cao, W. Yang, B. H. Xie, and M. B. Yang, Macromolecules **47**, 1439 (2014).
39. J. Wang, R. Lv, B. Wang, B. Na, and H. Liu, Polymer **143**, 52 (2018).
40. J. Shao, Y. Guo, S. Ye, B. Xie, Y. Xu, and H. Hou, Polym. Sci., Ser. A **59**, 116 (2017).
41. S. Saeidlou, M. A. Huneault, H. B. Li, P. Sammut, and C. B. Park, Polymer **53**, 5816 (2012).
42. Y. F. Huang, Z. C. Zhang, Y. Li, J. Z. Xu, L. Xu, Z. Yan, G. J. Zhong, and Z. M. Li, Cryst. Growth Des. **18**, 1613 (2018).
43. J. Shao, Y. Guo, S. Xiang, D. Zhou, X. Bian, J. Sun, G. Li, and H. Hou, CrystEngComm **18**, 274 (2016).
44. H. P. Chen, S. Nagarajan, and E. M. Woo, Macromolecules **53**, 2157 (2020).
45. Y. Guo, J. Shao, and H. Hou, J. Appl. Polym. Sci. **134**, e44730 (2017).
46. J. Zhang, K. Tashiro, H. Tsuji, and A. J. Domb, Macromolecules **41**, 1352 (2008).
47. J. Shao, Y. L. Liu, S. Xiang, X. C. Bian, J. R. Sun, G. Li, X. S. Chen, and H. Q. Hou, Chin. J. Polym. Sci. **33**, 1 (2015).
48. L. Wang, C. Feng, D. Zhou, J. Shao, H. Hou, and G. Li, Polym. Cryst. **1**, e10006 (2018).
49. L. Cartier, T. Okihara, and B. Lotz, Macromolecules **30**, 6313 (1997).
50. M. Avrami, J. Chem. Phys. **8**, 212 (1940).
51. M. Avrami, J. Chem. Phys. **7**, 1103 (1939).
52. C. S. Feng, Y. Chen, J. Shao, G. Li, and H. Q. Hou, Chin. J. Polym. Sci. **38**, 298 (2020).
53. H. Y. Yin, X. F. Wei, R. Y. Bao, Q. X. Dong, Z. Y. Liu, W. Yang, B. H. Xie, and M. B. Yang, CrystEngComm **17**, 2310 (2015).
54. X. Liu, C. Li, D. Zhang, and Y. Xiao, J. Polym. Sci., Part B: Polym. Phys. **44**, 900 (2006).